Supporting Information for

Crystalline silicon nanoparticles formation by tailored plasma irradiation: self-structurization, nucleation and growth accelerations, and size control

Daehan Choi[1,2], Jung Hyung Kim[1], Deuk Chul Kwon[3], Chae Ho Shin[1], Hyun Ryu[1], Euijoon Yoon[2], Hyo-Chang Lee[1,4]*

[1]Korea Research Institute of Standards and Science, Daejeon 34113, South Korea

[2]Department of Materials Science and Engineering, Seoul National University, Seoul 08826, South Korea

[3]National Fusion Research Institute, Gunsan 54004, South Korea

[4]Department of Electrical Engineering, Hanyang University, Seoul 04763, South Korea

*Correspondence and requests for materials should be addressed to H.-C. Lee (email: LHC@kriss.re.kr)

As-deposited a-Si film

Fig. S1 shows the cross-sectional view HRTEM image of the as-deposited a-Si film prepared by low pressure chemical vapor deposition (LPCVD) on a SiO_2/Si substrate. The TEM sampling was proceeded by Ga+ ion using focused ion beam (FIB) system (FEI, Helios Nano Lab) operated at 30 kV. The short-range order was observed in the a-Si film. The thickness of a-Si film was also measured by ellipsometer at 9 points on the wafer.

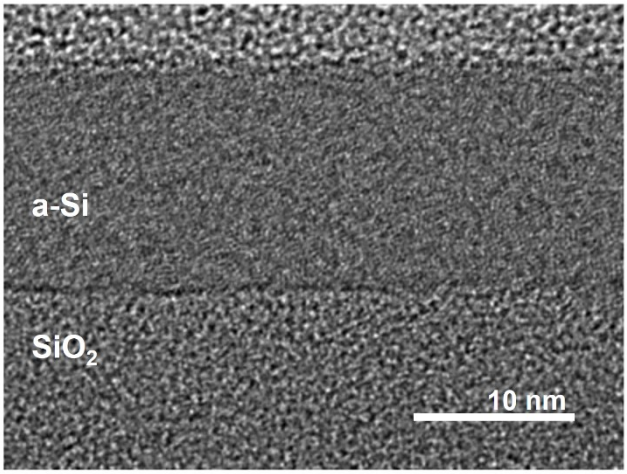

Average	*13.1358 nm*
Max thickness	*13.3389 nm*
Min thickness	*12.9984 nm*
Std. Dev.	*0.1072 nm*

Fig. S1. As-deposited a-Si film structure. High-resolution transmission electron microscope image of a 13-nm-thick a-Si film on SiO_2.

Figure 2 shows the Raman spectrum of as-deposited a-Si film. The broad band near 480 cm^{-1} indicates the a-Si structure with short range order[1,2].

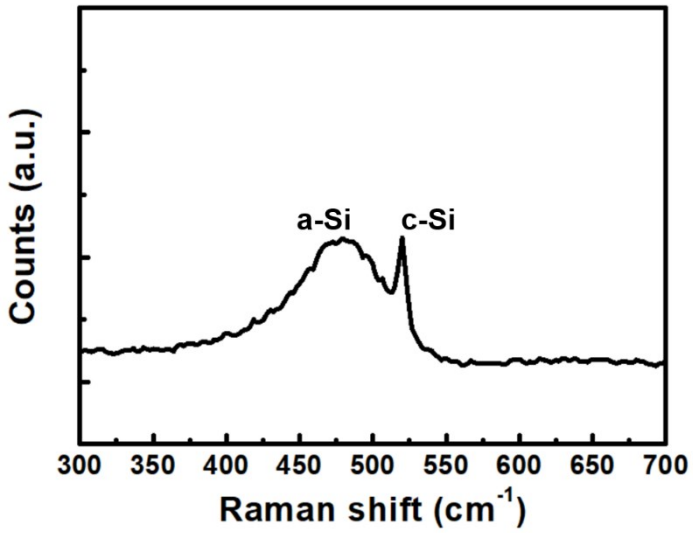

Fig. S2. As-deposited a-Si film composition. Raman spectrum of as-deposited 13-nm-thick a-Si film on SiO_2/Si substrate.

Conventional solid-state dewetting of a Cu thin film

Fig. S3 displays the Field-emission scanning electron microscope(FE-SEM) images of the conventional solid-state-dewetting process of a metal (Cu) film as a function of the inductively coupled plasma (ICP) treatment time. After plasma treatment for 10 min (**Fig. S3**b), long holes were generated, and Cu islands were formed in the entire film. According to the solid-state-dewetting theory,[3,4] grain boundaries can be hole-nucleation sites to separate the Cu film into islands. The dewetting of the film is proceeded not only near the surface, but also in the entire thickness region. With further plasma treatment for 1 h 20 min (**Fig. S3**c), the Cu islands were divided into Cu NPs. On the other hand, in the PTIS process (**Fig. 1**), the Si NSs were generated and their sizes grew by self-structurization at the surface, not the entire thickness region. This has many advantages in terms of mass production in industrial practical use because top-down or bottom-up process is possible in large area wafer-scales.

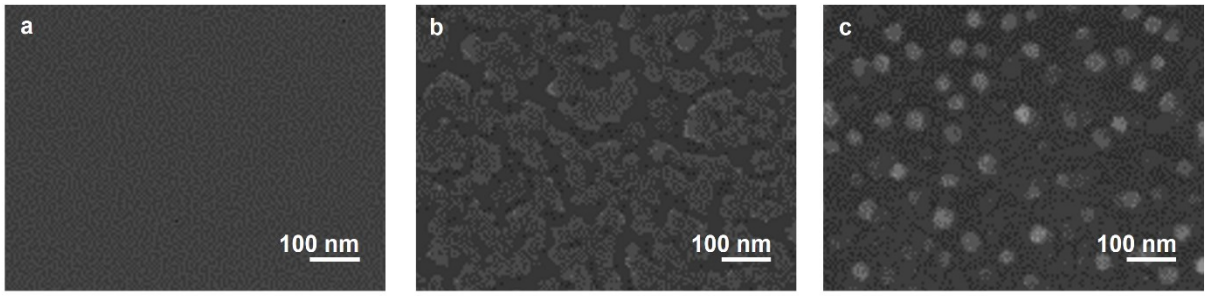

Fig. S3. Conventional metal dewetting for comparison with our method: **(a-c) a Cu film formed after ICP treatment depending on time:** (a) as-deposited, (b) 10 min, and (c) 80 min

Evolution of the Si NSs on the surface of a thicker a-Si film

Fig. S4 shows FE-SEM images of the formation of Si NPs by the PTIS process of a 30 nm-thick a-Si film. Although the thickness of the a-Si film is large, as the plasma treatment was proceeded, Si NSs were also generated on the surface (**Fig. S4**b) and grew in size (**Fig. S4**c). **The 30 nm thick a-Si film showed very similar size of Si NPs after plasma treatment compared to 13 nm thick a-Si film, which indicates the generation of NPs occurs near subsurface by crystallization mechanism. The plasma ion energy transferred to the surface induces nucleation and NPs grow larger. On the other hand, the annealing of 13 nm thick a-film and 30 nm thick a-film showed totally different results as shown in Fig. 3 of the manuscript.**

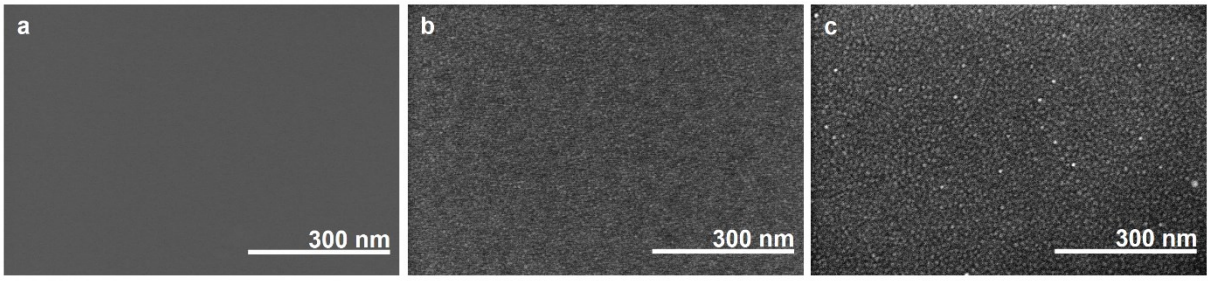

Fig. S4. Si NP creation at the surface (a-c) **a 30 nm-thick a-Si film after ICP treatment with a bias power of 9 W by times**: (a) as-deposited, (b) 10 min, and (c) 30 min**.**

Generation of C NPs on the surface of the amorphous carbon layer

Fig. S5 displays FE-SEM images of the amorphous carbon layer (ACL) before and after ICP treatment with ion energy of 43 eV for 10 min. The ACL was prepared on a Si wafer by plasma-enhanced chemical vapor deposition. The deposition of the ACL was performed using a gas mixture of C_2H_2 (250 sccm), He (500 sccm), Ar (1700 sccm), and N_2 (700 sccm) at a working pressure of 7 Torr. **Fig. S5**a shows the smooth surface morphology of the ACL film before the plasma treatment. **Fig. S5**b demonstrates the C NPs fabricated on the ACL through the surface structurization after the PTIS process.

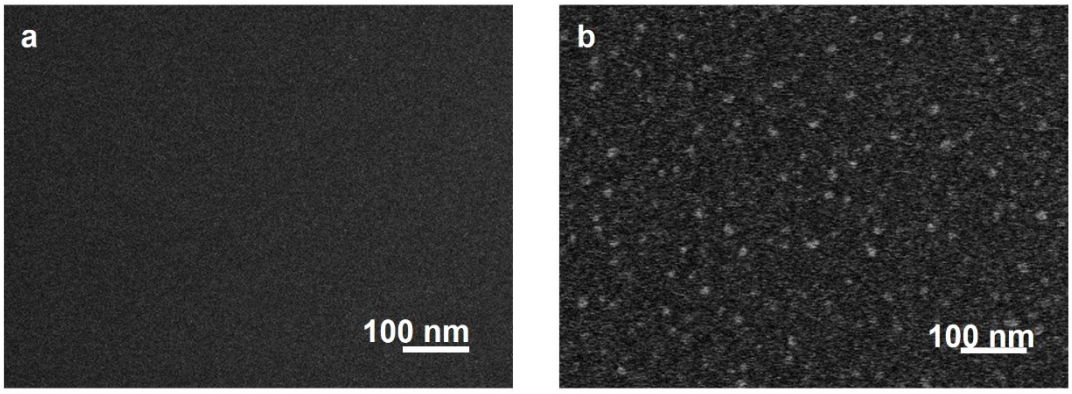

Fig. S5. (a, b) Carbon NP formation using PTIS: an amorphous carbon layer (a) before ICP treatment and (b) after ICP treatment with an ion energy of 43 eV for 10 min.

Confirmation of single crystallinity of Si NPs by HRTEM analysis

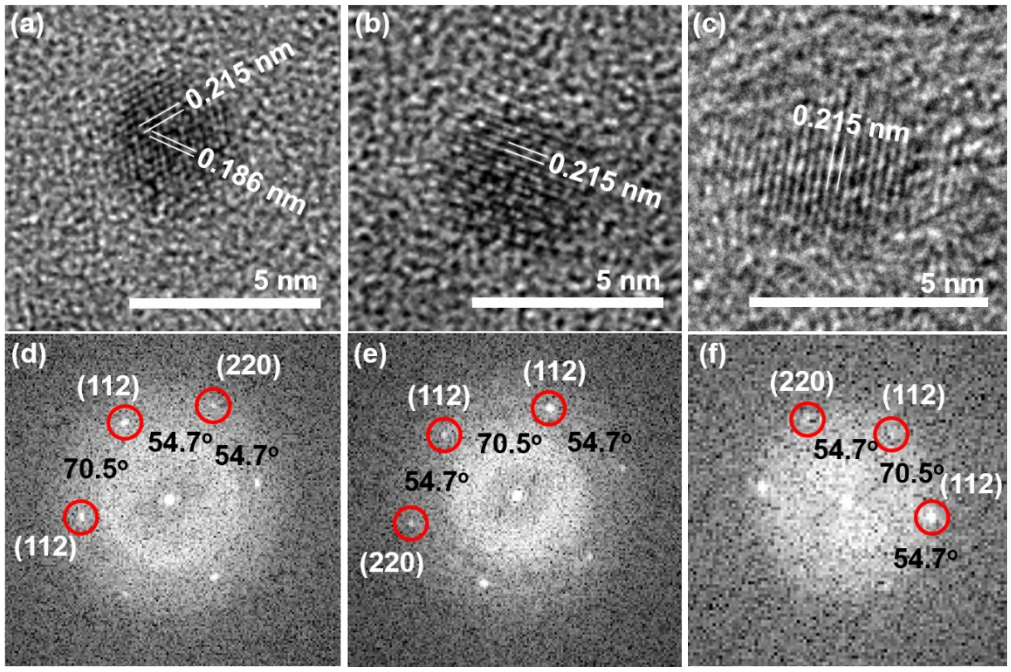

Fig. S6. HRTEM images and FFT patterns of Si NPs formed after plasma treatment at (a), (d) 9 W, 15 min, (b), (e) 9 W, 25 min, (c), (f) 11 W 15 min.

We measured plan-view HRTEM images of several spots of Si NPs and confirmed crystallinity of Si NPs. **Fig. S6**a-c indicates that Si NPs show single crystalline structure and have lattice plane spacing of diamond cubic Si. And **Fig.S6**d-f shows the characteristic interplanar angle of crystalline diamond cubic Si. Because the TEM sampling was carried out in the PIPS system (Gatan, PIPS II 695) to be thinned by low-energy (3 keV) Ar+ ion milling from the bottom of the substrate, the topside was not damaged by ion beams. Furthermore, the HRTEM image of a-Si shown in **Fig. S1** indicates that the crystallization by high energy electron beam did not occur during the HRTEM measurement in our measuring condition.

Comparison of the number density and size of the Si NPs on SEM and TEM images

Fig. S7a-c shows FE- SEM images of the Si NPs corresponding to the TEM images in **Fig 2**a-c. The number density and average size of the Si NPs on the FE-SEM and TEM images are compared in **Fig. S7**d and **S7**e. The number densities of the Si NPs were about 3.7 times higher on the TEM images than those on the SEM images for all plasma exposure times, which indicates that many Si NPs are embedded under the surface. The average size of the Si NPs was smaller by about 0.3 nm on the TEM images than on the SEM images, which can be due to the smaller size of the Si NPs embedded under the surface.

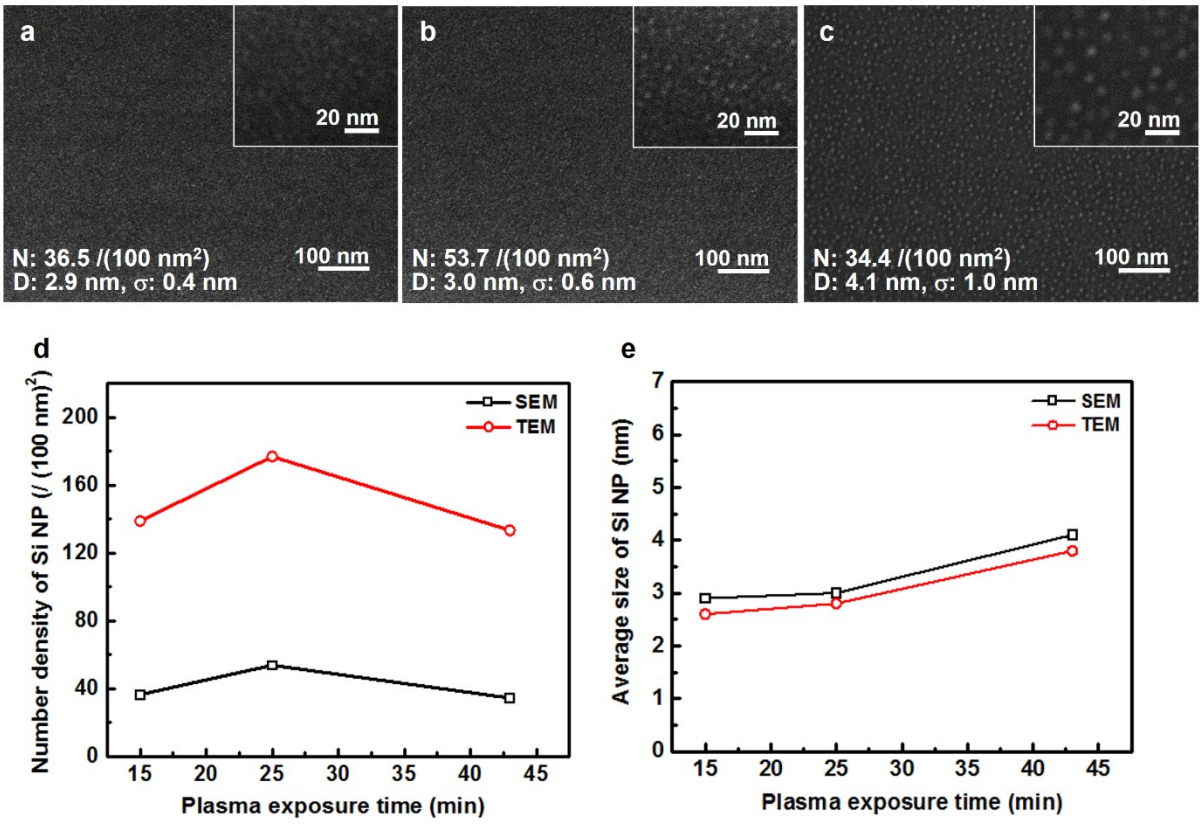

Fig. S7. Comparison with HRTEM image in the number density and size of the Si nanoparticles (NPs). (a-c) FE-SEM images of the Si NPs fabricated at an RF bias power of 9 W depending on the plasma exposure time: (a) 15, (b) 25, and (c) 43 min. (d) Number density and (e) average size of the Si NPs on the FE-SEM images (**Fig. S7**a-c) and TEM images (**Fig. 2**a-c).

Confirmation of the Si NP generation by nucleation due to the ion energy

Fig. S8 shows that the Si NPs are created by the nucleation process in the surface (also and subsurface region) owing to the ion energy induced by the RF bias power. **Fig. S8**a and **S8**b illustrate the schematics of ICP treatment without a bias (low ion energy) and with a bias power (high ion energy) of 9 W, respectively. When the RF bias power was not applied to the a-Si film where the ion transfer energy was insufficient, Si NPs were not generated (**Fig. S8**a). In the ICP treatment with the bias power (**Fig. S8**b), ions with higher energy are accelerated by a plasma sheath and bombard the a-Si surface to generate Si NPs. **Fig. S8**c and **S8**e show FE-SEM images of the a-Si film after ICP treatment without a bias. The change in the surface morphology was not observed after only ICP treatment for 10 min (**Fig. S8**c) and for 2 h 10 min (**Fig. S8**e).

In contrast, Si NSs were formed after ICP treatment with the bias (9 W) for 10 min (**Fig. S8**d). As shown in **Fig. S8**f, after the formation of NSs by ICP treatment with the bias (9 W) for 10 min, it was confirmed that the NP growth proceeded only by an additional ICP treatment without a bias for 2 h. This results indicate that tailoring the ion energy near the sputtering threshold energy can create a threshold energy required for the nucleation. This is a surface-control technology on the nucleation and crystallization physics.

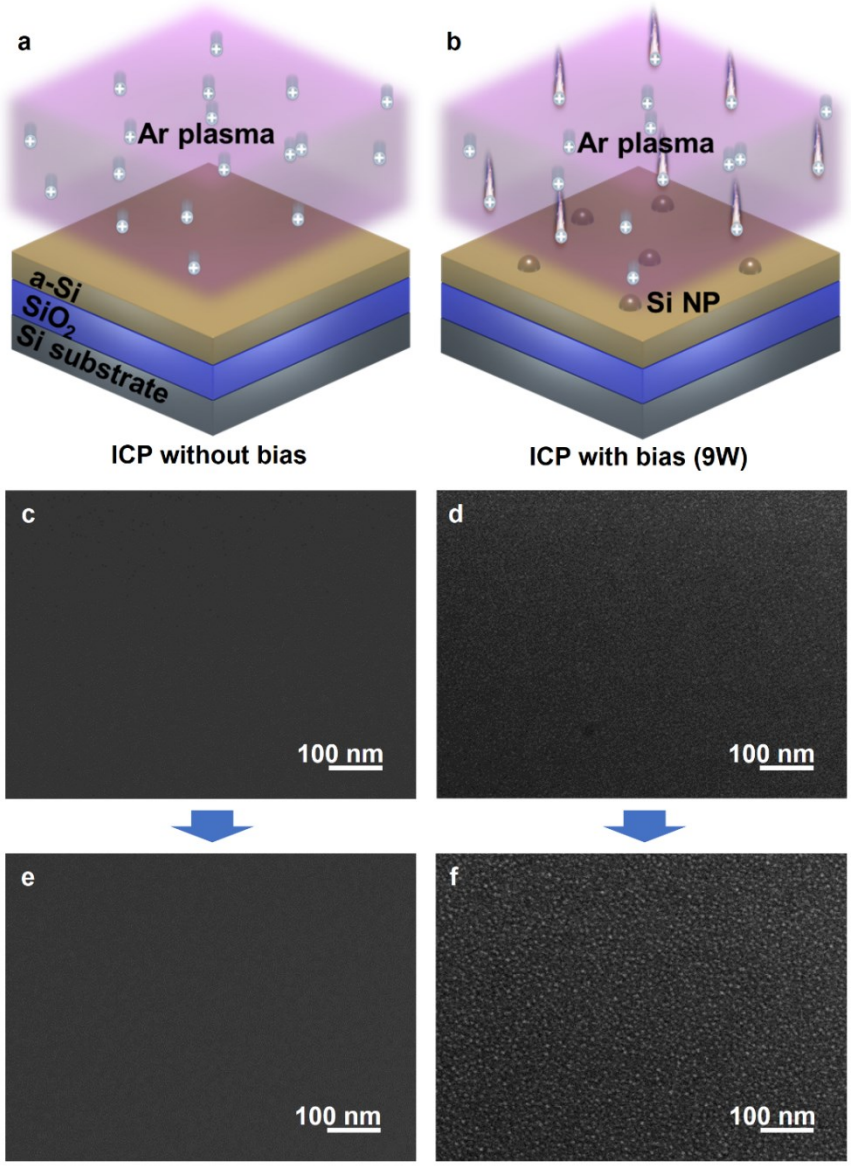

Fig. S8. Experimental evidence on the threshold energy for NP formation (a, b) Schematics of the ICP treatment on an a-Si film (a) without an RF bias and (b) with an RF bias power of 9 W. (c-f) the a-Si film after ICP treatment (c) without a bias for 10 min, (d) with a bias power of 9 W for 10 min, (e) without a bias for 2 h 10 min, and (f) with a bias power of 9 W for 10 min, then without a bias for 2 h.

Size distribution of Si NPs formed after PTIS process with different bias power

Fig. S9 displays the size distribution of Si NPs formed after plasma treatment for varying time with an RF bias power of 6, 7, and 9 W corresponding to **Fig. 4**a of manuscript. The histograms show that the size distribution is narrower with decreasing NP size.

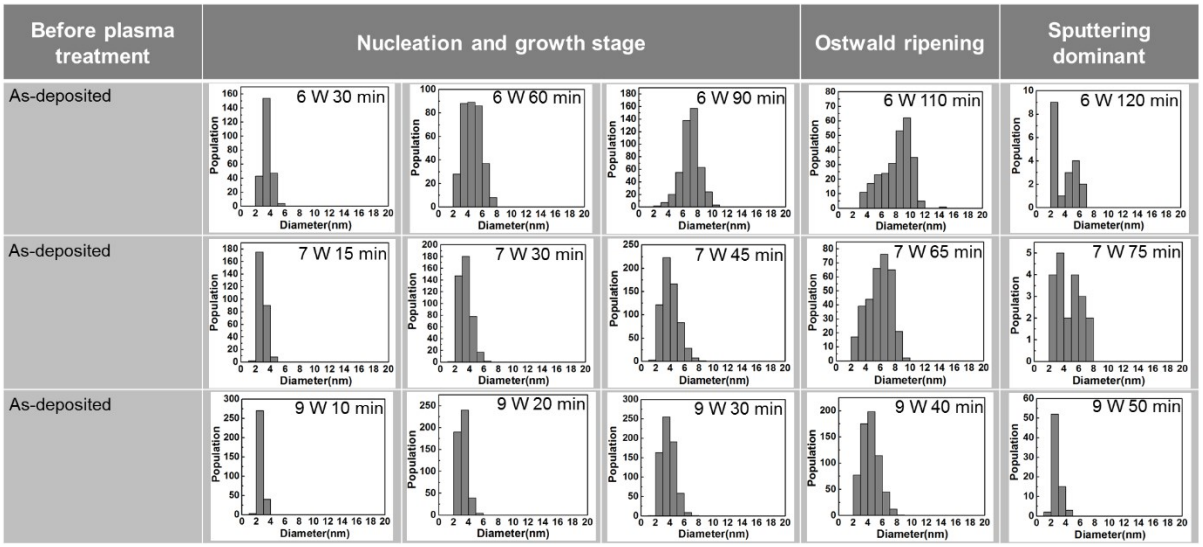

Fig. S9. Histograms of size distribution of Si NPs formed after plasma treatment depending on time with an RF bias power of 6, 7, and 9 W corresponding to **Fig. 4**a.

Different morphologies of the a-Si film after ICP etching with high-energy ions

Fig. S10 demonstrates FE-SEM images of the a-Si film after ICP treatment with a high ion energy above 135 eV. The separated valley structure was generated by bombarding ions with an energy of 135 eV (**Fig. S10**a), and the smooth surface was obtained by ions with an energy of 199 eV (**Fig. S10**b). The morphology evolution was totally different from the fabrication mechanism of the c-Si NPs under the optimal ion energy condition near the sputtering threshold energy, so called the PTIS method proposed in this work. Although the ion energy in **Fig. S10** was still significantly lower than that used in the ripple formation method,[5-13] it seems that the roughness increased because of the dependence of the sputtering yield on the curvature.[12,13]

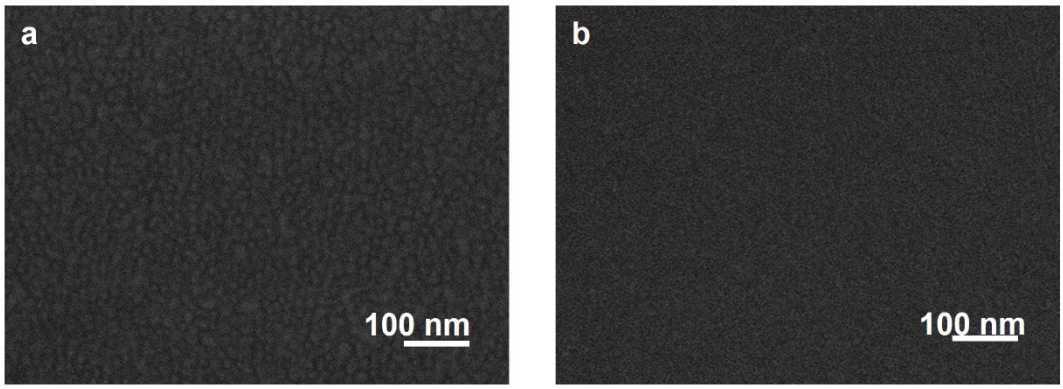

Fig. S10. Excessive plasma ion energy effect beyond the PTIS (a, b) an a-Si film after ICP treatment (a) with an ion energy of 135 eV for 3 min and (b) with an ion energy of 199 eV for 1 min.

RF biased ICP chamber structure and sample location

Fig. S11 illustrates the schematic of RF biased ICP chamber used for the formation of Si NPs. The a-Si film sample was loaded on the center of chuck. The Ar plasma treatment was performed.

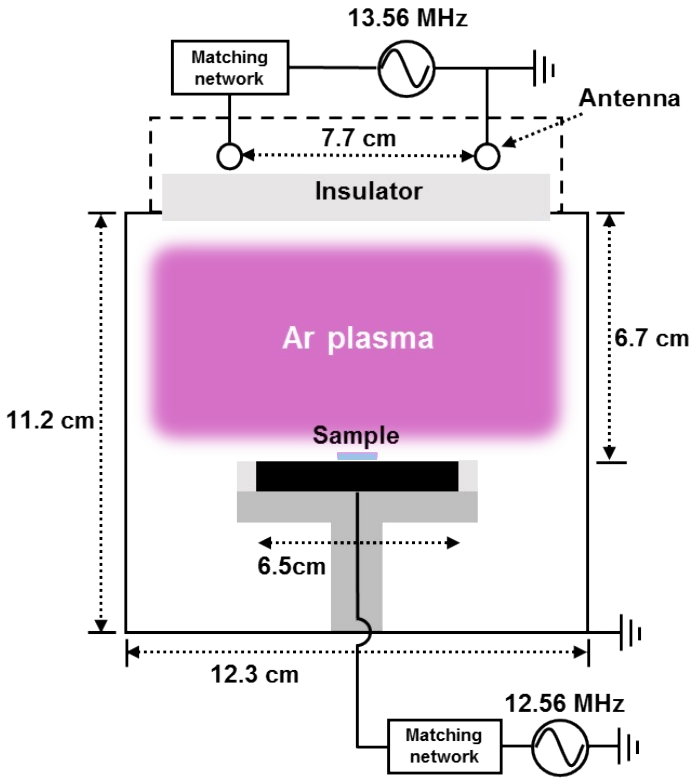

Fig. S11. Schematic diagram of the RF biased ICP chamber used for generation of Si NPs by PTIS method.

REFERENCES

(1) F.D. Heinz, W. Warta, and M.C. Schubert, *Energy Procedia*, 2012, **27**, 208-213.

(2) S. Park, B. Parida, K. Kim, *J. Nanosci. Nanotechnol.*, 2013, **13**, 1-6.

(3) E. C. Neyts, K. Ostrikov, Z. J. Han, S. Kumar, A. C. T. Van Duin, A. Bogaerts, *Phys. Rev. Lett.,* 2013, **110**, 065501.

(4) M. Naffouti, T. David, A. Benkouider, L. Favre, A. Ronda, I. Berbezier, S. Bidault, N. Bonod, M. Abbarchi, *Nanoscale,* 2016, **8**, 2844-2849.

(5) J. Muñoz-García, L. Vázquez, M. Castro, R. Gago, A. Redondo-Cubero, A. Moreno-Barrado, R. Cuerno, *Mater. Sci. Eng. R,* 2014, **86**, 1-44.

(6) B. Ziberi, F. Frost, B. Rauschenbach, T. Höche, *Appl. Phys. Lett.,* 2005, **87**, 033113.

(7) G. Ozaydin, A. S. Özcan, Y. Wang, K. F. Ludwig, H. Zhou, R. L. Headrick, D. P. Siddons, *Appl. Phys. Lett.,* 2005, **87**, 163104.

(8) J. Muñoz-García, R. Gago, R. Cuerno, J. A. Sánchez-García, A. Redondo-Cubero, M. Castro, L. Vázquez, *J. Phys.: Condens. Matter,* 2012, **24**, 375302.

(9) R. Gago, L. Vázquez, R. Cuerno, M. Varela, C. Ballesteros, J. M. Albella, *Appl. Phys. Lett.,* 2001, **78**, 3316-3318.

(10) D. Chowdhury, D. Ghose, B. Satpati, *Mater. Sci. Eng. B,* 2014, **179**, 1-5.

(11) B. Ziberi, F. Frost, T. Höche, B. Rauschenbach, *Phys. Rev. B,* 2005, **72**, 235310.

(12) R. M. Bradley, J. M. E. Harper, *J. Vac. Sci. Technol. A,* 1988, **6**, 2390-2395.

(13) W. L. Chan, E. Chason, *J. Appl. Phys.,* 2007, **101**, 121301.